International Journal of Engineering

Chemical Synthesis of Zinc Oxide Nanoparticles with Nanorod and Spherical Morphologies

E. Darezereshki[a], A. B. Vakylabad[b], M. Yousefi*[a]

[a] Department of Materials Engineering, Shahid Bahonar University of Kerman, Kerman, Iran
[b] Department of Materials, Institute of Science and High Technology and Environmental Sciences ,Graduate University of Advanced Technology, Kerman, Iran

P A P E R   I N F O

A B S T R A C T

ZnO nanoparticles were prepared by direct thermal decomposition of the precursor [contain: $Zn_4(SO_4)(OH)_6.H_2O$ and ZnO] in air for 1 h at 875°C. The pH of the precursor solution was set at 6 and 11 by the controlled addition of the $NH_3·H_2O$ solution. The as-prepared materials were characterized by X-ray diffraction (XRD), infrared spectrum (FTIR), scanning electron microscopy (SEM), and transmission electron microscopy (TEM). According to the analyses, the ZnO nanoparticles were pure with both rod-like and spherical shapes which were synthesized using chloride and sulfate solutions, respectively. Moreover, the average diameter of synthesized spherical ZnO at pH=6 was around 85±5 nm; while, an average diameter of the nanorods was 980 nm and 2.2 μm in length. The average nanorods diameter at pH=11 was 760 nm and 3.3 μm in length; while the average particle size of spherical shape was around 112±5 nm. The TEM and SEM image showed the morphology of spherical and nanorods particles. The reaction temperature of all steps during the synthesis of ZnO nanopowders shifted to high temperature, as the pH of the starting solution increased from 6 to 11. Due to the simplicity, the present method could be proposed as a convenient approach to produce pure ZnO nanoparticles by means of $ZnSO_4$ and $ZnCl_2$ solutions without using any toxic and organic chemicals.

doi: 10.5829/ije.2021.34.08b.10

1. INTRODUCTION

Zinc oxide (ZnO) is an important material for applications in catalytic luminescent and electronic (e.g., varistors, semiconductors, and gas sensors) devices, pigments, rubber, ceramics, chemical and components for the pharmaceutical and cosmetic industries [1-4]. Additionally, ZnO nanostructures were used as nanoadsorbent to remove heavy metals that the removal efficiency depends on the shapes of ZnO nanoparticles [5, 6]. Different morphologies of ZnO including nanospheres, nanorods, nanoflowers, nanotubes, nanoplates and nanotripods have been reported [7]. The literature showed that microstructures and chemical properties of ZnO depend on the synthesis method, synthesis parameters, and also the used starting

precursor. Different synthesis methods were used to prepare ZnO particles of different size and morphology. Table 1 summarized a description of different morphologies obtained under various synthesis conditions and methods [8-21]. Among these methods, precipitation and thermal decomposition are low cost techniques which can provide large scale production without expensive raw materials and complicated equipment. Moreover, different zinc salts such as zinc acetate dehydrate $(Zn(C_2H_3O_2)_2·2H_2O))$, zinc nitrate hexahydrate $(Zn(NO_3)_2·6H_2O)$ zinc sulfate $(Zn(SO_4)_2·7H_2O)$ and zinc chloride $(ZnCl_2)$ as precursor have been used. ZnO nanoparticles prepared using $Zn(NO_3)_2·6H_2O$ precursor was mixture of nano-prisms and nanorods shape with an average crystallite size of 18.91 nm [22].

Synthesis of ZnO crystalline-structures from $ZnSO_4$ solution with carbonate solutions such as Na_2CO_3, NH_4HCO_3, etc. often leads to the occurrence of a

* Corresponding Author Institutional Email: *m.yousefi@eng.uk.ac.ir* (M. Yousefi)

TABLE 1. Methods for preparing ZnO nano-structures with different size and morphologies

Reaction	Explanation	Reference
$Zn_4SO_4(OH)_6.xH_2O \rightarrow ZnSO_4.3Zn(OH)_2$ xH_2O $2[ZnSO_4.3Zn(OH)_2 \rightarrow 5ZnO + Zn_3O(SO_4)_2 + 6H_2O$ $Zn_3O(SO_4)_2 \rightarrow 3ZnO + 2SO_2 + O_2$	Chemical reaction at 70 °C to form the precursor of $Zn_4(SO_4)(OH)_6 \cdot 0.5\ H_2O$, then, thermal decomposition for the synthesis of ZnO nanoparticles in air for 1 h at 825 °C, with the 92 nm nanoparticles.	[8]
$Zn_2B_6O_{11} + 3H_2O \rightarrow Zn_2B_6O_{11} + 3H_2O$ (at room temperature) $Zn_2B_6O_{11} \rightarrow (900°C)\ 2ZnO + 3B_2O_3$	Decomposing zinc borate nanoplatelets at 900°C, average diameters of perfect spherical shape of nanoparticles was 50 nm.	[9]
$Zn(NH3)_4^{2+} + 2OH^- \rightarrow ZnO + 4NH_3 + H_2O$	Transformation of $Zn(NH3)_4^{2+}$ complexes as a precursor in the presence of sodium oleate and hydrazine at 80 °C, ZnO nanoparticles with 30–60 nm	[10]
$Zn(CH_3COO)_2 + 2NaOH \rightarrow Zn(OH)_2 + 2CH_3COONa$ $Zn(OH)_2 \rightarrow$ Hydrothermal $ZnO + H_2O$	Hydrothermal method at 100-200°C for different periods from 5 - 10 h, nano-particles size of ZnO in the range of 55–110 nm	[11]
$Zn^{2+} + 2OH^- \rightarrow Zn(OH)_2$ $Zn(OH)_2 \rightarrow ZnO + H_2O$ $Zn(OH)_2 + 2OH^- + TEA \rightarrow [Zn(OH)4]^{2-}TEA$ 	Aqueous solution of zinc acetate dehydrate ($Zn(CH_3COO)_2 \cdot 2H_2O$, 0.1 M) and 2.0 mL of triethanolamine (TEA) as a surfactant; 1 M ammonia (NH_4OH) as a reduction agent. Hydrothermal treatments at 95 °C for 2 h. ZnO microcrystals with length of 2.2 μm and diameter of 1.8 μm, a single crystal wurtzite structure.	[12]
$NH_3.H_2O \rightarrow NH_4^+ + OH^-$ $Zn^{2+} + 2OH^- \rightarrow Zn(OH)_2$ $Zn(OH)_2 + 2OH^- \rightarrow Zn(OH)_4^{2-}$ $Zn(OH)_2 + 4NH_3.H_2O \rightarrow [Zn(NH_3)_4]^{2+} + 2OH^- + 4H_2O$ $[Zn(NH_3)_4]^{2+} + 4H_2O \rightarrow ZnO + 3NH_4^+ + 2NH_3.H_2O$ $Zn(OH)_4^{2-} \rightarrow ZnO + H_2O + 2OH^-$	Hydrothermal process at 180°C for 20 h. uniform pencil-like crystals with the average diameter of 300 nm and length of about 10 μ*m*	[13]
$ZnSO_4 + 2NH_4OH \rightarrow Zn(OH)_2 + (NH_4)_2SO_4 \rightarrow ZnO\ (s) + 4NH_3(aq) + 2H_2O(l)$	Synthesized through a novel low-temperature aqueous solution route (90–95°C) and rapid thermal processing (300-850°C). One-dimensional (1D) ZnO nanorod arrays and branched two-dimensional (2D), three-dimensional (3D) – nanoarchitectures.	[14]
$Zn(CH_3COO)_2 + H_2O \rightarrow ZnO + 2CH_3COOH$ $HOCH_2CH_2OH \leftrightarrow CH_3CHO + H2O$ $CH_3CHO + 2AgNO_3 + H_2O \rightarrow 2Ag + 2HNO_3 + CH_3COOH$	Fabrication of the Ag/ZnO microspheres via a ''one-pot'' process in ethylene glycolmedium. heating the solution to 160 °C at the rate of 5 °C/min.	[15]
$C_6H_{12}N_4 + 6H_2O \rightarrow 6CH_2O + 4NH_3$ $NH_3 + H_2O \rightarrow NH^{4+} + OH^-$ $Zn(CH_3COO)_2 + 2NH^{4+} + 2OH^- \rightarrow 2CH_3COONH_4 + Zn(OH)_2$ $Zn^{2+} + 2OH^- + 2H_2O \rightarrow Zn(OH)_4^{2-} + 2H^+$ $Zn(OH)_4^{2-} + 2H^+ \rightarrow ZnO_{cluster} + 3H_2O$	The chemical growth of ZnO nanorod arrays in the solution on the ITO substrates by a two- step chemical bath deposition (CBD) method with an average of 1.83 μm in length and 87 nm in diameter. The reaction temperature from 25 to 95 °C	[16]
$Zn_5(CO_3)_2(OH)_6 \rightarrow 5ZnO + 3H_2O\uparrow + 2CO_2\uparrow$	Precipitation of the precursor using $ZnCl_2$ and Na_2CO_3 by heating; calcinations at 300-400°C. Mean sizes of nano-particles, ranging from 8 nm to 80 nm.	[17]
$CO(NH_2)_2(s) + 3H_2O(l) \rightarrow CO_2(g) + 2NH_3.H_2O(aq)$ $2NH_3-H_2O(aq) + CO_2(g) \rightarrow 2NH_4^+(aq) + CO_3^{2-}(aq)$ $NH_3.H_2O(aq) \rightarrow NH_4^+\ (aq) + OH^-(aq)$ $Zn^{2+}(aq) + CO_3^{2-}(aq) + 4OH^-\ (aq) + 3H_2O(l)$ $\rightarrow ZnCO_3.2Zn(OH)_2.H_2O(s)$ $ZnCO_3.2Zn(OH)_2.H_2O(s) \rightarrow 3ZnO(s) + 3H_2O(g) + CO_2(g)$	The industrial preparation of ZnO nanoparticles using a stirring tank reactor containing the zinc nitrate solution under 95 °C conditions, direct precipitation method.	[18]
$5ZnSO_4(aq) + 10NH_4HCO_3(aq) \rightarrow Zn_5(CO_3)_2(OH)_6(s)) + 5(NH_4)_2SO_4(aq) + 8CO_2(g) + 2H_2O(l)$ $Zn_5(CO_3)_2(OH)_6(s) \rightarrow 5ZnO(s) + 2CO_2(g) + 3H_2O(g)$	direct precipitation method at room temperature; precursor dried at 100°C, and calcinations at 300, 350, 400, and 500° C. ZnO nano-particles with average crystal size of about 9.4 nm	[19]
$(CH_2)_6N_4 + 6H_2O \rightarrow 6HCHO + 4NH_3$ $NH_3 + H_2O \rightarrow NH_4OH^-$ $Zn^{2+} + 2OH^- \rightarrow ZnO + H_2O$	Totally 20 cycles for the deposition of ZnO nanorods at 95°C. The well-defined hexagonal facet, the side length of about 150 nm, the aspect ratio of 2:3.	[20]
$Zn^{2+} + 4NH_3 \rightarrow Zn(NH_3)_4^{2+}$ $Zn(NH_3)_4^{2+} + 2OH^- \rightarrow ZnO + 4NH_3 + H_2O$	First, reaction of the Zn ions in $Zn(NO_3)_2.6H_2O$ solution with ammonia to form amine complexes ($Zn(NH_3)_4^{2+}$), second, reaction of the complex with OH^- to produce ZnO crystals; hydrothermal growth of the ZnO nanorods in an oven at 90°C for 1–3 h.	[21]

carbonate compound of Zn as precursor $[Zn_5(CO_3)(OH)_6]$ [23]. Depending on the concentration of the precursor, the nanostructures prepared through breakdown and recombination of ionic bonds [24] may exhibit itself in composition of ZnO particles. For instance, $ZnCl_2$ as precursor results in a mixture of ZnO and $Zn_5(OH)_8Cl_2.H_2O$ phases [22]. The presence of these phases in the final product indicates that the conversion of reactants into the desired ZnO product is not complete. However, it is established that different zinc salts have little or no effects on the crystallite size of ZnO nanoparticles [5].

Precise control of the size and shape of nanocrystals results in desired chemical and physical properties [25]. In hydrothermal synthesis, the effect of pH is crucial because OH^- is strongly related to the series of reactions that produced ZnO [26, 27]. The flower-like ZnO nanostructures are synthesized by decomposing $Zn(OH)_2$ in which the zinc nitrate is used as a precursor. The size of the ZnO is altered with pH of the solution [7]. In addition, the reaction temperature and the concentration of salt precursors play a critical role in the crystallite size [28]. There is still considerable uncertainty regarding the factors affecting end-product properties and the mechanism by which the high purity ZnO nanoparticles form within a simple and cost-effective method.

Herein, we report an innovative and simple method to synthesize ZnO nano-structures through thermal decomposition of the precursor [contain: $Zn_4(SO_4)(OH)_6 \cdot H_2O$ and ZnO] which prepared at the room temperature from $ZnSO_4$, $ZnCl_2$ and NH_4OH. The preparation procedure is to be conducted without using any organic and toxic solvents. Among many parameters affecting the nanostructures' growth, the pH of the precursor preparation is to be investigated in relation to the morphological changes of the ZnO nanostructures. Moreover, changes in dimensions as the pH changes are also expected to be observed.
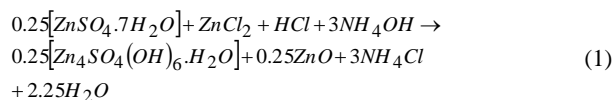
2. MATERIALS AND METHOD

All of the reagents used in these experiments including zinc sulfate heptahydrate ($ZnSO_4 \cdot 7H_2O$), zinc chloride ($ZnCl_2$), ammonium solution (NH_4OH), hydrochloric acid (HCl) and ethanol (CH_3CH_2OH) were of analytical grade. All these starting chemicals were supplied by Merck Chemicals Company (Darmstadt, Germany). Distilled water was used as solvent. Precursor powders were synthesized using the following methods:

First, $ZnCl_2$ and $ZnSO_4 \cdot 7H_2O$ were dissolved in a 2 M hydrochloric acid to form a solution with the concentration of 2 M for $ZnCl_2$ and 1 M for $ZnSO_4 \cdot 7H_2O$. After complete mixing by a magnetic

stirrer, the $NH_3 \cdot H_2O$ solution (1 M (final pH=6.12) and 2 M (final pH=11.23)) dropwise added to the solution with vigorous mixing at room temperature for 2 h. The obtained precursor, the preparation pH of which was 6.12 will be referred hereafter as "precursor #1", and that was 11.23 will be named as "precursor #2". The obtained ZnO powders after calcinations of them will be referred hereafter as "powder #1" (from precursor #1) and "powder #2" (from precursor #2).

The white precipitate precursors (1 and 2) were collected by filtration. They were then rinsed four times with deionized water and absolute ethanol; then, dried at 70 °C overnight. In the precipitation process, the ZnO powder was formed according to Equation (1):

$$0.25[ZnSO_4.7H_2O] + ZnCl_2 + HCl + 3NH_4OH \rightarrow$$
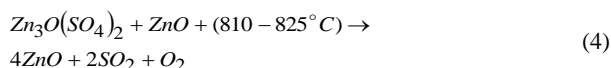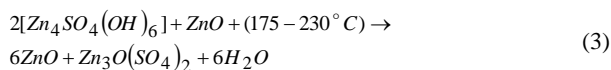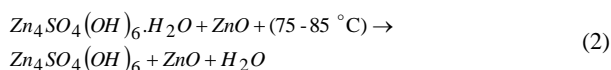$$0.25[Zn_4SO_4(OH)_6.H_2O] + 0.25ZnO + 3NH_4Cl \qquad (1)$$
$$+ 2.25H_2O$$

Finally, the precursors were calcinated in a muffle furnace at 875 °C for 1 h under atmospheric air pressure. The crystalline structure of the nanoparticles was characterized by X-Ray diffraction (XRD, PHILIPS, X'pert-MPD system) using Cu Kα (λ=1.54 A°) radiation. The thermal behavior of the precursors was studied by thermogravimetry (TG), under air flow. 35 mg of samples were heated with the heating rate of 10 °C/min at temperature range of 35–900 °C. Infrared (IR) spectra were recorded on a Bruker tensor 27 Fourier Transform infrared (FTIR) spectrometer with RTDLATGS detector, in the range of 400 to 4000 cm^{-1} with a spectral resolution of 4 cm^{-1} in transmittance mode. The morphology and average particle size of ZnO nanoparticles were also determined with scanning electron microscopy (SEM, Tescan Vega-II) and a transmission electron microscopy (TEM, PHILIPSCM20).

3. RESULTS AND DISCUSSIONS

Figure 1 (a and b) shows the TG-DSC analysis for the prepared precursors at pH=6.12 and pH=11.23 in the air flow, respectively. Three endothermic peaks (75.5 °C and 85°C; 175.5°C and 230 °C; 810 °C and 825 °C) were found in the heating process. The peaks correspond to the crystal water decomposition reaction (Equation (2)), dehydroxylation of the basal hydroxide layer (Equation (3)), and the decomposition of sulfate groups (Equation (4)). Due to the large number of disk-like $Zn_4SO_4(OH)_6$ in the precursor at pH=11.23, temperature of dehydroxylation of the basal hydroxide layer (230 °C) was higher than the precursor at pH=6.12 (175 °C).

In the decomposition process, the white powder ZnO was formed from the following reactions [Equations (2)-(4)]:

$$Zn_4SO_4(OH)_6.H_2O + ZnO + (75\text{-}85\ ^{\circ}C) \rightarrow$$
$$Zn_4SO_4(OH)_6 + ZnO + H_2O \tag{2}$$

$$2[Zn_4SO_4(OH)_6] + ZnO + (175-230^{\circ}C) \rightarrow$$
$$6ZnO + Zn_3O(SO_4)_2 + 6H_2O \tag{3}$$

$$Zn_3O(SO_4)_2 + ZnO + (810-825^{\circ}C) \rightarrow$$
$$4ZnO + 2SO_2 + O_2 \tag{4}$$

The results confirmed the scheme of decomposition [8,14,19], including the three sequential stages, which led to the formation of ZnO as the final product.

These reactions were governed by the pH of the solution. As observed by increasing the pH, the reaction temperature of all steps during the synthesis of ZnO nano-powders shifted to the higher temperature.

Figure 2 shows X-ray diffraction patterns of the precursor #1 (a), precursor #2 (b), ZnO powder #1, (c), and the powder #2 (d). All the diffraction peaks in Figures 2a and 2b are consistent with the $Zn_4SO_4(OH)_6.H_2O$ phase (JCPDS card no. 00-039-0690) and hexagonal phase ZnO which was reported in JCPDS card (No. 00-036-1451). As summarized in Table 2, the ZnO nano-rods which was prepared from the precursor synthesized at pH=6.12, displayed the stronger diffraction peaks than pH=11.23. It revealed that the nano-rods pertaining to pH=6.12 possessed well-aligned growth and high crystal quality [29-32]. Moreover, the crystallinity of ZnO nanostructures was improved after annealing.
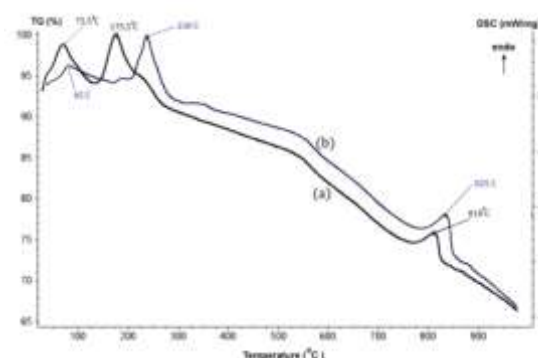

Figure 1. TGA–DSC curves of the ZnO precursors prepared at (a) pH=6 and (b) pH=11 from 35 to 900 ˚C
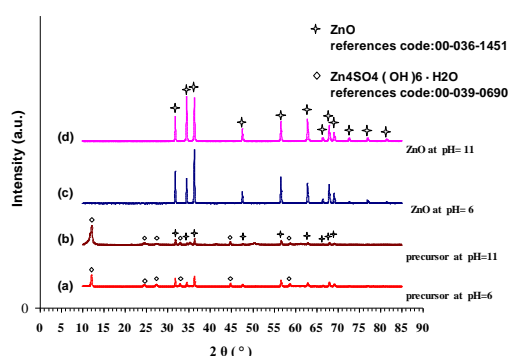

Figure 2. X-ray patterns of the precursor #1 (a), precursor #2 (b), ZnO powder #1 (c), and powder #2 (d) synthesized by direct thermal decomposition of the precursors at 875 °C for 1 h

TABLE 2. Representative X-ray of Zinc oxide powder diffraction data in the prepared precursor at pH=6.12 and pH=11.23

h	k	l	ZnO crystals in the synthesized precursor at pH= 6.12			ZnO crystals in the synthesized precursor at pH=11.23		
			$d_{cal.}$	$d_{meas.}$	Peak height (cts)	$d_{cal.}$	$d_{meas.}$	Peak height (cts)
1	1	0	2.811	2.814	431	2.810	2.814	261
0	0	2	2.601	2.603	196	2.599	2.603	90
1	0	1	2.474	2.476	518	2.472	2.475	292
1	0	2	1.910	1.911	92	1.907	1.911	39
1	1	0	1.624	1.625	310	1.624	1.624	194
1	0	3	1.477	1.477	162	1.476	1.477	77
2	0	0	1.406	1.407	52	1.406	1.407	29
1	1	2	1.378	1.378	187	1.378	1.378	92
2	0	1	1.358	1.358	110	1.358	1.358	66
0	0	4	1.303	1.301	13	1.305	1.301	3
2	0	2	1.238	1.238	26	1.239	1.238	22
1	0	4	1.184	1.181	10	1.186	1.181	9.6

Disk and hexagonal shapes of $Zn_4SO_4(OH)_6 \cdot H_2O$ and ZnO, respectively, were detected in the SEM images (Figure 3). The stability of zinc hydroxy-sulfate decreases in acidic conditions (pH<7) [33], which leads to more ZnO precipitating from the solution phase. As shown in Figure 3 (a, b) and (c, d), the amount of hexagonal rod shapes of ZnO in the precursor #1 are more than the precursor #2, which agrees well with the XRD analysis.

According to the FTIR spectra shown in Figure 4(A), the absorption peaks at 441, 597.68, 961.74, and 1125.93 cm^{-1} are attributed to SO_4^{2-} and 417 cm^{-1} is assigned to ZnO [8,34]. The peak at 769.73 cm^{-1} is the stretching mode of Zn-OH vibrations. The results of IR analyses confirmed that the produced precursor was $Zn_4SO_4(OH)_6 \cdot H_2O$ and ZnO, that is in agreement with the results of XRD. When the precursors were heated at 875 °C for 1 h, they decomposed into ZnO crystallite phase (JCPDS card no. 00-036-1451) (Figure 2 c and d). In this case, the ZnO nano-crystals were hexagonal with the lattice parameters: a = 3.24 Å, b = 3.24 Å, c = 5.20 Å (space group= $P6_3mc$). Representative X-ray ZnO powder diffraction data are shown in Table 3. Sharp peaks indicated elevated crystallinity of ZnO. Figure 4(B) shows the FTIR spectrum of the ZnO nano-powders prepared through thermal decomposition at 875°C. The absorption band at 430.06 and 507.45 cm^{-1} (Figure 4B) are attributed to Zn–O, and the band at 3428.27 cm^{-1} is attributed to –OH stretching [34]. The

band at 1635.99 cm^{-1} is due to the OH bending of water. Finally, the tiny dip in the spectra at 2369.67 cm^{-1} is due to atmospheric CO_2 [35-38]. In general, the IR peaks intensities at pH=6.12 are higher than those at pH=11.23. It could be postulated that the higher IR peaks intensity are due to the higher ZnO structures particles during the thermal decomposition [39]. The average diameter and the length of the nanorods in the powder #1 were 980 nm and 2.2 μm, respectively; while, in the powder #2, the diameter and length were 760 nm and 3.3 μm, respectively. Generally, the aspect ratio of the ZnO nanorods increased with the enhanced concentration of OH^-. It is worth noting that an increase in concentration of OH^- ions could partially suppress the growth of as-deposited ZnO nanocrystallines [16]. Thus, the diameter of nanorods decreased when the concentration of OH^- increased from pH 6.12 to 11.23 (see Figure 5).

Figures 6 and 7 show TEM images of powder #1 and powder #2, respectively. Figures 8a and 9a show that the spherical ZnO nanoparticles have a wide size distribution with the average diameter of 85±5 nm and 112±5 nm, respectively. The Rosin–Rammler (RR) distribution function (Equation (5)) is the most commonly used equation for describing the particle size distribution (PSD) [40]:
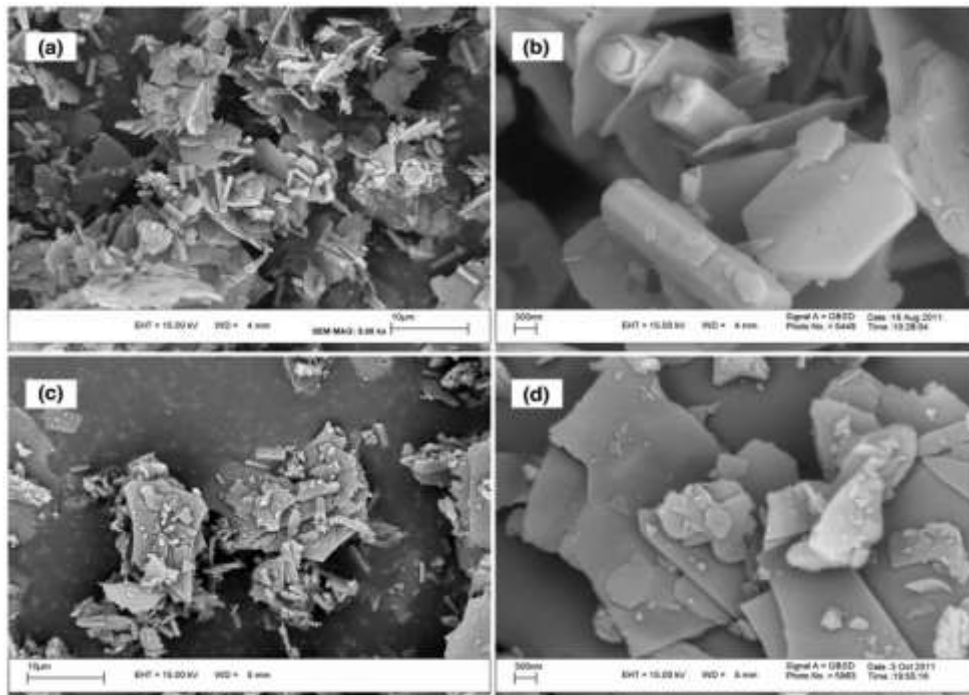
$$Q(x) = 1 - \exp\left[-(x/d_0)^n\right] \tag{5}$$

Figure 3. SEM images of the (a, b) precursor #1 (prepared at pH=6), and (c, d) precursor #2 (prepared at pH=11) at two different magnifications
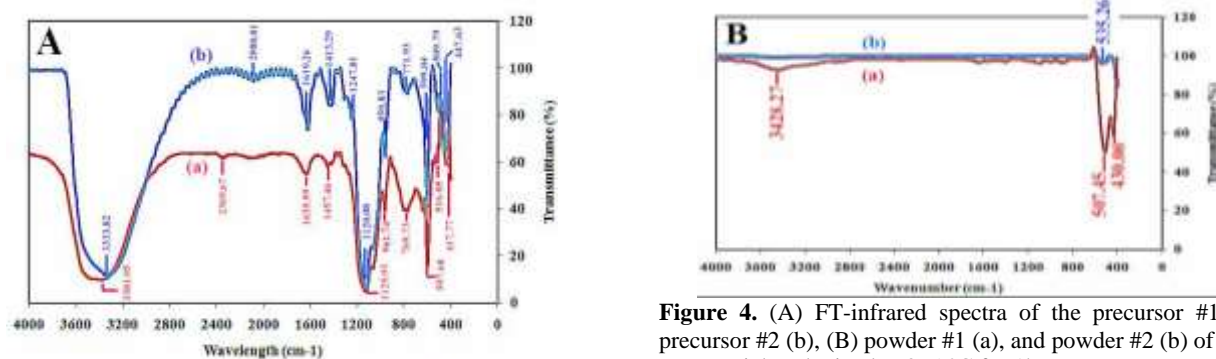
Figure 4. (A) FT-infrared spectra of the precursor #1 (a), precursor #2 (b), (B) powder #1 (a), and powder #2 (b) of ZnO nanoparticles obtained at 875 °C for 1h

TABLE 3. Representative X-ray Zinc oxide powder (#1 and #2) diffraction data

| h	k	l	ZnO crystals in powder #1			ZnO crystals in powder #2		
			$d_{cal.}$	$d_{meas.}$	Peak Height [cts]	$d_{cal.}$	$d_{meas.}$	Peak Height [cts]
1	1	0	2.812	2.814	1569	2.812	2.814	1204
0	0	2	2.601	2.603	1193	2.600	2.603	2180
1	0	1	2.474	2.475	2615	2.474	2.476	2096
1	0	2	1.910	1.911	575	1.910	1.911	599
1	1	0	1.623	1.624	1284	1.623	1.625	959
1	0	3	1.476	1.477	956	1.476	1.477	1063
2	0	0	1.406	1.407	202	1.406	1.407	151
1	1	2	1.377	1.378	918	1.377	1.378	741
2	0	1	1.357	1.358	502	1.357	1.358	396
0	0	4	1.300	1.301	84	1.300	1.301	144
2	0	2	1.237	1.238	151	1.237	1.238	135
1	0	4	1.180	1.181	73	1.180	1.181	90
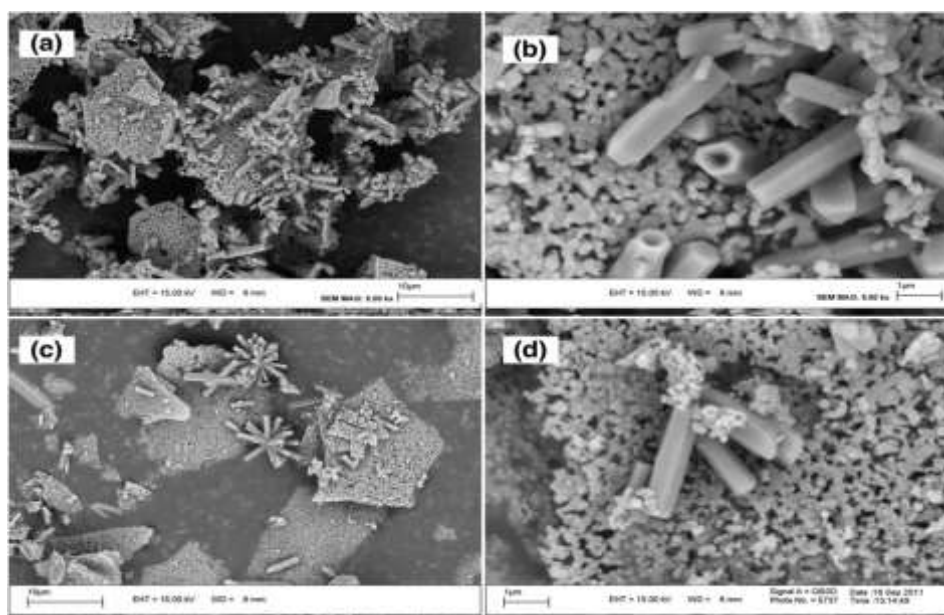
Figure 5. SEM images of (a, b) powder #1 (prepared at pH=6), and (c, d) powder #2 (prepared at pH=11) at two different magnifications
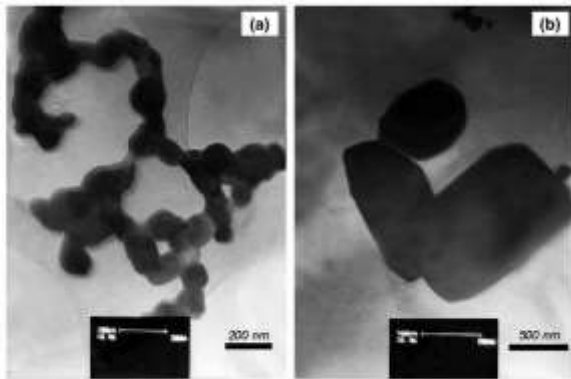
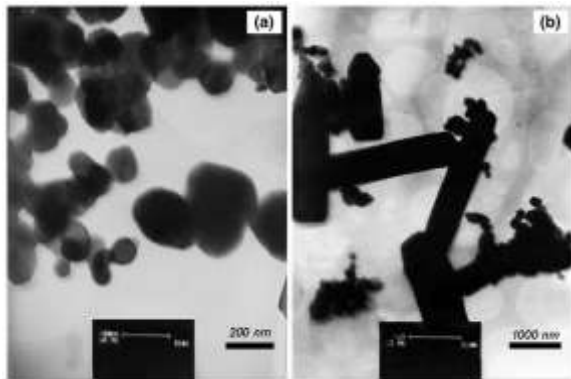**Figure 6.** TEM images of the ZnO nano-architectures (powder #1)

Figure 7. TEM images of the ZnO nano-architectures (powder #2)

dominate as the temperature of the reaction is increased in this series of reactions by increasing pH value (Figure 1). According to Figures 8, 9 and Table 4, the lower n values in both powders indicate the wider particle-size distributions [40].
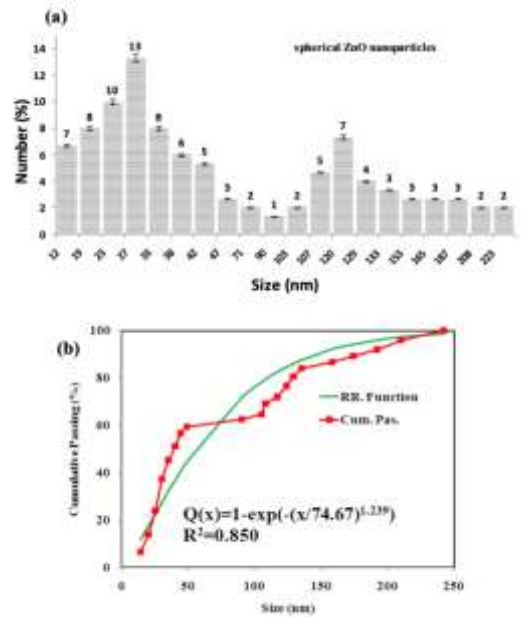

Figure 8. (a) Particle size distribution and (b) fitting of the Rosin–Rammler equation into the ZnO nanospheres of powder #1 data by using TEM analysis
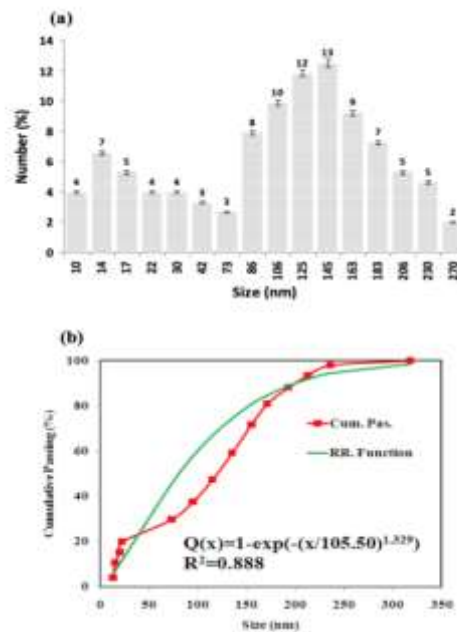

Figure 9. (a) Particle size distribution and (b) fitting of the Rosin–Rammler equation into the ZnO nanospheres of powder #2 data by using TEM analysis

where, x is the measured particle size, $Q(x)$ is the cumulative fraction passing function, d_0 is the size factor, and n is the spread factor. The size factor, d_0, is a characteristic of the PSD. In the function, the size factor indicates the fineness of powder. So, the smaller d_0, the finer is the powder. On the other hand, the spread factor, n, is a measure of the uniformity. It is larger for narrower distribution. That is, the higher the n value the more uniform is the distribution.

The parameters of the PSD of the sphere-like ZnO by using the Rosin–Rammler model is illustrated in Table 4. The factor of d_0 is 74.67 for the spheres of powder #1 while it is 106.50 for powder #2. It indicated that the average size of the sphere-like particles of the ZnO in powder #1 was lower than that of powder #2. It established a direct relationship between the reaction temperature and particle sizes. Increasing the reaction temperature leads to either an increase in the formation of nuclei, which would promote smaller particles in the end-product, or a faster rate of decomposition of zinc-hydroxo- complexes to ZnO, which results in the growth and coarsening of the end-products [33]. In this case, however, the growth of particles seems to

TABLE 4. Rosin–Rammler equation parameters for TEM data from spherical ZnO nanoparticles

Factor	Powder	
	Powder #1	Powder #2
d_0	74.67	106.50
n	1.239	1.329

4. CONCLUSIONS

Pure ZnO nanoparticles have been successfully produced with a simple thermal decomposition method without using organic solvents, expensive raw materials, and complicated equipment. Then, the SEM and TEM images showed that the ZnO nanoparticles were of rod and spherical shapes. The following major conclusions were made.

- The sequential occurrence of ZnO nanoparticles was included nanorods and nanosphere. Nanorods were obtained in the earliest stage when $ZnCl_2$ was used as a zinc ion source, which implied that the source of Zn ions affected the morphology of the synthesized ZnO nanoparticles.
- The average particles size of ZnO nanoparticles increased with increasing pH of the reaction media.
- As the pH of the starting solution increased from 6 to 11, the reaction temperature of all steps during the synthesis of ZnO nanopowders including the water decomposition, dehydroxylation and decomposition of sulfate groups were shifted to the higher amounts.
- A direct relationship was observed between the reaction temperature and particle sizes. As if, raising the reaction temperature increased the average particle size of ZnO.
- The diffraction peaks decreased in intensity with the increasing pH value.

  Finally, the facile protocol can be proposed for synthesis of zinc oxide nano-materials with rod and spherical shapes. Again, future programs have been designed to control the operational parameters to obtain ZnO nano-structures with desired size, shape, and alignment.

5. ACKNOWLEDGEMENTS

6. REFERENCES

1.   Gondal, M.A., Drmosh, Q.A., Yamani, Z.H. and Saleh, T.A., "Synthesis of ZnO_2 nanoparticles by laser ablation in liquid and their annealing transformation into ZnO nanoparticles", *Applied Surface Science*, Vol. 256, (2009), 298-304, doi: 10.1016/j.apsusc.2009.08.019

2.   [2] Bigdeli, F. and Morsali, A., "Synthesis ZnO nanoparticles from a new Zinc(II) coordination polymer precursor", *Materials Letters*, Vol. 64, (2010), 4-5, doi: 10.1016/j.matlet.2009.09.038

3.   [3] Music, S., Drag, D., Popovic, S. and Ivanda. M., "Precipitation of ZnO particles and their properties", *Materials Letters*, Vol. 59, (2005), 2388-2393, doi: 10.1016/j.matlet.2005.02.084

4.   Janet Priscilla, S., Andria Judi, V., Daniel R. and Sivaji, K., "Effects of Chromium Doping on the Electrical Properties of ZnO Nanoparticles", *Emerging Science Journal,* Vol. 4, (2020), 82-88, doi: 10.28991/esj-2020-01212

5.   Shaba, E.Y., Jacob, J.O., Tijani, J.O. and Suleiman, M.A.T., "A critical review of synthesis parameters affecting the properties of zinc oxide nanoparticle and its application in wastewater treatment", *Applied Water Science,* Vol. 11, (2021), 1-41, doi: 10.1007/s13201-021-01370-z

6.   Durguti, V., Aliu, S., Laha, F. and Feka, F., "Determination of Iron, Copper and Zinc in the Wine by FAAS", *Emerging Science Journal,* Vol. 4, (2020), 411-417, doi: 10.28991/esj-2020-01240

7.   Heidari, A., Younesi, H. and Zinatizadeh, A.A.L., "Controllable Synthesis of Flower-like ZnO Nanostructure with Hydrothermal Method", *International Journal of Engineering Transactions B: Applications*, Vol. 22, (2009), 283-290.

8.   Darezereshki, E., Alizadeh, M., Bakhtiari, F., Schaffie, M. and Ranjbar, M., "A novel thermal decomposition method for the synthesis of ZnO nanoparticles from low concentration $ZnSO_4$ solutions", *Applied Clay Science*, Vol. 54, (2011), 107-111, doi: 10.1016/j.clay.2011.07.023

9.   Tian, Y., Ma, H., Shen, L., Wang, Z., Qu, Y. and Li, Sh., "Novel and simple synthesis of ZnO nanospheres through decomposing zinc borate nanoplatelets" *Materials Letters*, Vol. 63, (2009), 1071-1073, doi: 10.1016/j.matlet.2009.02.009

10.   Li, M., Bala, H., Lv, X., Ma, M., Sun, F., Tang, L. and Wang, Z., "Direct synthesis of monodispersed ZnO nanoparticles in an aqueous solution", *Materials Letters*, Vol. 61, (2007), 690-693, doi: 10.1016/j.matlet.2006.05.043

11.   Ismail, A.A., El-Midany, A., Abdel-Aal, E.A. and El-Shall, H., "Application of statistical design to optimize the preparation of ZnO nanoparticles via hydrothermal technique", *Materials Letters*, Vol. 59, (2005), 1924-1928, doi: 10.1016/j.matlet.2005.02.027

12.   Zeng, Y., Zhang, T. and Qiao, L., "Preparation and gas sensing properties of the nutlike ZnO microcrystals via a simple hydrothermal route", *Materials Letters*, Vol. 63, (2009), 843-846, doi: 10.1016/j.matlet.2009.01.012

13.   Dai, K., Zhu, G, Liu, Z., Liu, Q., Chen, Z. and Lu, L., "Facile preparation and growth mechanism of zinc oxide nanopencils", *Materials Letters*, Vol. 67, (2012), 193-195, doi: 10.1016/j.matlet.2011.09.079

14.   Lupan, O., Chow, L., Chai, G., Roldan, B., Naitabdi, A., Schulte, A. and Heinrich, H., "Nanofabrication and characterization of ZnO nanorod arrays and branched microrods by aqueous solution route and rapid thermal processing", *Materials Science and Engineering B*, Vol. 145, (2007), 57-66, doi: 10.1016/j.mseb.2007.10.004

15.   Tian, C., Li, W., Pan, K., Zhang, Q., Tian, G., Zhou, W. and Fu, H., "One pot synthesis of Ag nanoparticle modified ZnO microspheres in ethylene glycol medium and their enhanced photocatalytic performance", *Journal of Solid State Chemistry*, Vol.183, (2010), 2720-2725, doi: 10.1016/j.jssc.2010.09.020

16. Lee, Y.M. and Yang, H.W., "Optimization of processing parameters on the controlled growth of ZnO nanorod arrays for the performance improvement of solid-state dye-sensitized solar cells", *Journal of Solid State Chemistry*, Vol. 184, (2011), 615-623, doi: 10.1016/j.jssc.2011.01.021

17. Han, Y.X., Ding, Y.Z., Yin, W.Z. and Ma, Z.X., "Preparation of homogeneous ZnO nanoparticles via precipitation-pyrolysis with $ZnS(CO_3)_2(OH)_6$ as precursor", *Transactions Nonferrous Metals Society of China*, Vol. 16, (2006), 1205-1212, doi: 10.1016/S1003-6326(06)60402-0

18. Wang, Y., Zhang, Ch., Bi, S. and Luo, G., "Preparation of ZnO nanoparticles using the direct precipitation method in a membrane dispersion micro-structured reactor", *Powder Technology*, Vol. 202, (2010), 130-136, doi: 10.1016/j.powtec.2010.04.027

19. Wang, Y., Zhang, C., Bi, S. and Luo, G., "Preparation of ZnO nanoparticles using the direct precipitation method in a membrane dispersion micro-structured reactor", *Powder Technology*, Vol. 202, (2010), 130-136, doi: 10.1016/j.powtec.2010.04.027

20. Gao, X.D., Li, X.M., Yu, W.D., Li, L. and Qiu, J.J., "Seed layer-free synthesis and characterization of vertically grown ZnO nanorod array via the stepwise solution route", *Applied Surface Science*, Vol. 253, (2007), 4060-4065, doi: 10.1016/j.apsusc.2006.09.002

21. Lee, D., Yoo, M., Seo, H., Tak, Y., Kim, W.G., Yong, K., Rhee, S.W. and Jeon, S., "Enhanced mass sensitivity of ZnO nanorod-grown quartz crystal microbalances", *Sensors and Actuators B*, Vol. 135, (2009), 444-448, doi: 10.1016/j.snb.2008.10.026

22. Gusattia, M., Barrosoa G.S.,, Maduro de Camposb, C.E., Souza, D.A. and Rosário, J.A., "Effect of Different Precursors in the Chemical Synthesis of ZnO Nanocrystals", *Materials Research,* Vol. 14, (2011), 264-267, doi: 10.1590/S1516-14392011005000035

23. Alhawi, T, Rehana, M, York, D and Lai, X., "Hydrothermal Synthesis of Zinc Carbonate Hydroxide Nanoparticles", *Procedia Engineering,* Vol. 102, (2015), 356 - 361, doi: 10.1016/j.proeng.2015.01.158

24. Trang, G.T.T., Linh, N.H., Linh, N.T.T. and P. H. Kien,"The Study of Dynamics Heterogeneity in SiO_2 Liquid", *HighTech and Innovation Journal,* Vol. 1, (2020), 1-7, doi: 10.28991/HIJ-2020-01-01-01

25. Gharibshahian, E., "The Effect of Polyvinyl Alcohol Concentration on the Growth Kinetics of $KTiOPO_4$ Nanoparticles Synthesized by the Co-precipitation Method", *HighTech and Innovation Journal,* Vol. 1, (2020), 187-193, doi: 10.28991/HIJ-2020-01-04-06

26. Jaejin, S, Seonghoon, B., Jonghyuck, L. and Sangwoo, L., "Role of OH− in the low temperature hydrothermal synthesis of ZnO nanorods", *Journal of Chemical Technology and Biotechnology*, Vol. 83, (2008), 345-350, doi: 10.1002/jctb.1817

27. Zare, E., Pourseyedi, Sh., Khatami, M. and Darezereshki, E., "Simple biosynthesis of zinc oxide nanoparticles using nature's source, and it's in vitro bio-activity", *Journal of Molecular Structure*, Vol. 1146, (2017), 96-103, doi: 10.1016/j.molstruc.2017.05.118

28. Purwaningsih, S.Y., Zainuri, M., Triwikantoro, T., Pratapa, S. and Darminto, D., "Structural, Optical and Defect State Analyses of ZnO Nanoparticle Films", *International Journal of Engineering Transactions B: Applications,* Vol. 33, (2020), 852-860, doi: 10.5829/ije.2020.33.05b.17

29. Liang, H.Q., Pan, L.Z. and Liu, Z.J., "Synthesis and photoluminescence properties of ZnO nanowires and nanorods by thermal oxidation of Zn precursors", *Materials Letters*, Vol. 62, (2008), 1797-1800, doi: 10.1016/j.matlet.2007.10.010

30. Li, Z., Huang, X., Liu, J., Li, Y. and Li, G., "Morphology control and transition of ZnO nanorod arrays by a simple hydrothermal method", *Materials Letters*, Vol. 62, (2008), 1503-1506, doi: 10.1016/j.matlet.2007.09.011

31. Wang, M., Na, E.K., Kim, J.S., Kim, E.J., Hahn, S.H., Park, C. and Koo, K.K., "Photoluminescence of ZnO nanoparticles prepared by a low-temperature colloidal chemistry method", *Materials Letters*, Vol. 61, (2007), 4094-4096, doi: 10.1016/j.matlet.2007.01.026

32. Chang, W.Y., Fang, T.H., Weng, C.I. and Yang, S.S., "Flexible piezoelectric harvesting based on epitaxial growth of ZnO", *Applied Physics A: Materials Science & Processing*, Vol. 102, (2011), 705-711, doi: 10.1007/s00339-010-5962-z

33. Moezzi, A., Cortie, M. and McDonagh A., "Aqueous pathways for the formation of zinc oxide nanoparticles", *Dalton Transactions.*, Vol. 40, (2011), 4871-4878, doi: 10.1039/C0DT01748E

34. Darezereshki, E., Behrad Vakylabad, A. and Koohestani, B.,"A Hydrometallurgical Approach to Produce Nano-ZnO from Electrical Arc Furnace Dusts", *Mining, Metallurgy & Exploration*, (2021), 1-11, doi: 10.1007/s42461-021-00412-z

35. [35] Darezereshki, E., "One-step synthesis of hematite (α-Fe_2O_3) nano-particles by direct thermal-decomposition of maghemite", *Materials Letters*, Vol. 65, (2011), 642-645, doi: 10.1016/j.matlet.2010.11.030

36. Darezereshki, E., "Synthesis of maghemite (γ-Fe_2O_3) nanoparticles by wet chemical method at room temperature", *Materials Letters*, Vol. 64, (2010), 471-1472, doi: 10.1016/j.matlet.2010.03.064

37. Mostafaei, A. and Zolriasatein, A., "Synthesis and characterization of conducting polyaniline nanocomposites containing ZnO nanorods", *Progress in Natural Science: Materials International*, Vol. 22, No. 4, (2012), 273-280, doi: 10.1016/j.pnsc.2012.07.002

38. Darezereshki, E. and Bakhtiari, F., "A novel technique to synthesis of tenorite (CuO) nanoparticles from low concentration $CuSO_4$ solution", *Journal of Mining and Metallurgy, Section B: Metallurgy*, Vol. 47, No. 1, (2011), 73-78, doi: 10.2298/JMMB1101073D

39. Koohestani, B., Darban, AK., Mokhtari, P., Darezereshki, E., Yilmaz, E., and Yilmaz, E., "Influence of hydrofluoric acid leaching and roasting on mineralogical phase transformation of pyrite in sulfidic mine tailings", *Minerals*, Vol. 10, No. 6, (2020), 513-527, doi: 10.3390/min10060513

40. Darezereshki, E., Bakhtiari, F., Alizadeh, M., Behrad Vakylabad, A. and Ranjbar, M., "Direct thermal decomposition synthesis and characterization of hematite (a-Fe_2O_3) nanoparticles", *Materials Science in Semiconductor Processing,* Vol. 15, (2012), 91-97, doi: 10.1016/j.mssp.2011.09.009

Persian Abstract

چکیده

نانوذرات اکسید روی از طریق فرایند تجزیه حرارتی مستقیم پیش ماده [شامل: $Zn_4(SO_4)(OH)_6.H_2O$ و ZnO] در هوا به مدت ۱ ساعت و در دمای ۸۷۵ درجه سانتی‌گراد سنتز شدند. مقدار pH محلول از طریق افزودن محلول $NH_3.H_2O$ روی دو مقدار ۶ و ۱۱ تنظیم شد. مشخصه یابی نمونه‌ها با استفاده از آنالیز پراش پرتو ایکس (XRD)، طیف سنجی مادون قرمز (FT-IR) ، میکروسکوپ الکترونی روبشی (SEM) و میکروسکوپ الکترونی عبوری (TEM) انجام شد. نتایج نشان داد نانو ذرات خالص اکسید روی، با دو مورفولوژی کروی و میله ای، به ترتیب در محلول‌های کلریدی و سولفاتی تشکیل شدند. میانگین قطر نانوذرات کروی ZnO که از تجزیه حرارتی پیش ماده تهیه شده در pH = ۶ سنتز شد، حدود ۸۵ ± ۵ نانومتر بود، در حالی که نانومیله‌های ZnO به طور میانگین دارای قطر ۹۸۰ نانومتر و طول ۲/۲ میکرومتر بودند. در شرایط pH = ۱۱ نانومیله‌ها دارای قطر میانگین ۷۶۰ نانومتر و طول ۳/۳ میکرومتر بوده، در حالی که اندازه ذرات متوسط نانوذرات با مورفولوژی کروی حدود ۱۱۲ ± ۵ نانومتر بود. تصاویر حاصل از SEM و TEM حضور نانو ذرات میله‌ای و کروی را نشان داد. با افزایش pH محلول از ۶ به ۱۱ دمای واکش مربوط به تمام مراحل ساخت نانوذرات ZnO افزایش یافت. با توجه به نتایج حاصل، روش حاضر می‌تواند به عنوان روشی ارزان و مناسب برای تولید نانوذرات ZnO خالص با استفاده از محلول‌های $ZnSO_4$ و $ZnCl_2$ و بدون استفاده از هرگونه مواد شیمیایی سمی و آلی اعمال شود.